

# Adaptation of a 2-D Clinostat for Simulated Microgravity Experiments with Adherent Cells

Peter Eiermann · Sascha Kopp · Jens Hauslage ·  
Ruth Hemmersbach · Rupert Gerzer ·  
Krassimira Ivanova

Received: 17 January 2013 / Accepted: 3 May 2013 / Published online: 2 June 2013  
© Springer Science+Business Media Dordrecht 2013

**Abstract** The fast-rotating 2-D clinostat, a ground-based facility for investigations in simulated microgravity, is mainly used for experiments with cell suspensions. Here, we describe the adaptation of a 2-D clinostat for adherent cell investigations using commercially available slide flasks. As a gradient of residual accelerations is present in the slide flasks during clinorotation, the range of maximal *g*-values has to be adjusted to the investigated cells and type of analysis. For gene expression analysis, a harvesting slide chamber was constructed, allowing collection of cells exposed to defined *g*-values. Using this slide chamber, human 1F6 melanoma cell line, exposed in the ranges of  $\leq 0.012$  g,  $\leq 0.024$  g, or  $\leq 0.036$  g for 24 h, was harvested and the respective mRNA levels of guanylyl cyclase A (GC-A), an enzyme catalyzing cyclic GMP synthesis, were determined by real-time quantitative PCR analysis. Our results show that the down-regulation of GC-A mRNA levels in 1F6 melanoma cells depends on the residual acceleration values with a maximal reduction at  $\leq 0.012$  g. We further used the slide flasks by the clinorotation of murine RAW 264.7 macrophage cell line for f-actin analysis. The laser scanning microscopy images of cells exposed to *g*-values of  $\leq 0.006$  g for 1 h show an increase in the cell size of clinorotated cells, but no rearrangement in the f-actin filament system compared to static 1-g controls. Thus, 2-D clinostats equipped with slide flasks can be used for adherent cell experiments, however, the maximal *g*-values have to be carefully considered.

**Keywords** Adherent cells · Clinostat · Gene expression · Gravity · Melanoma cells · Slide flasks

## Introduction

Gravity is an environmental factor being present on earth. Many (unicellular) organisms have developed mechanisms to sense the gravity vector for orientation purposes. It has been demonstrated that mammalian cells react to hyper- or microgravity by changes in gene expression and cellular function (Hughes-Fulford and Lewis 1996; Ivanova et al. 2004, 2011; Ulbrich et al. 2011; Thiel et al. 2012). However, experimental capacities in real microgravity are limited due to high cost and rare access (International Space Station, ISS) and due to the short experimental time in the range of seconds to minutes (sounding rockets, drop tower). Therefore, parabolic flights (with repetitive changes of microgravity and hypergravity phases) or ground-based facilities (aiming to achieve conditions of simulated microgravity) are often used to investigate biological samples under altered gravity conditions, which in turn provide a prerequisite for experiments intended to be flown in space.

Fast-rotating 2-D clinostats are commonly used ground-based facilities for exposition of biological samples (small animals and plants, cells, and microorganisms) to simulated microgravity conditions. These are able to generate high quality of reduced gravity conditions ( $\geq 0.001$  g) and several studies have shown that results from various model systems using 2-D clinorotation are similar to results found in real microgravity (Hemmersbach et al. 2006; Brungs et al. 2011; Thiel et al. 2012; Herranz et al. 2013), thereby justifying the use of the term “simulated microgravity conditions”. In a fast-rotating 2-D clinostat, the sample is mounted

P. Eiermann · S. Kopp · J. Hauslage · R. Hemmersbach ·  
R. Gerzer · K. Ivanova (✉)  
Institute of Aerospace Medicine, German Aerospace Center  
(DLR), Linder Hoehe, 51147 Cologne, Germany  
e-mail: krassimira.ivanova@dlr.de

horizontally and rotated around an axis perpendicular to the gravity vector (Briegleb 1967), thereby preventing particle sedimentation. Suspensions of cells can easily be clinorotated by pipetting them in compartments of a sufficient small diameter. For exposition of adherent cells on a fast-rotating 2-D clinostat, there are limitations mainly due to the inverse correlation between the amount of cells (growth area) and the residual accelerations with respect to the quality of microgravity simulation. The values of the residual accelerations in the cell cuvette during rotation depend on the rotation speed (rotations per minute, rpm) and the rotation radius ( $r$ ) (Klaus et al. 1998), thereby restricting the experimental possibilities on 2-D clinostats.

Here, we describe the adaptation of adherent cells on a 2-D clinostat using commercially available slide flasks. For cell collection a special slide chamber has been constructed.

## Material and Methods

### Cell Culturing

As example for experiments with adherent cells using fast-rotating 2-D clinostats, we selected the low-metastatic human 1F6 melanoma cell line, which we have used in a previous 2-D clinostat study (Ivanova et al. 2011) and the murine RAW 264.7 macrophage cell line (Raschke et al. 1978). Pigmented 1F6 human melanoma cells (a kind gift from Prof. van Muijen, Department of Pathology, Nijmegen University, The Netherlands) were grown in Dulbecco's modified Eagle's medium (DMEM), containing 10 % (vol./vol.) heat-inactivated fetal calf serum (FCS), 2 mM glutamine, and antibiotics as described previously (Ivanova et al. 1997). Adherent murine RAW 264.7 cells were cultured in DMEM medium supplemented with 10 % FCS (vol./vol.) and 1 % penicillin/streptomycin. All cells were grown in incubators at 37 °C, 5 % CO<sub>2</sub>, and 97 % relative humidity.

### Clinorotation

The fast-rotating 2-D clinostat used in this study was originally developed by Briegleb (1992) and modified by J. Hauslage for the use of slide flasks (Fig. 1a). It provides two parallel horizontal clinorotation axes, each for fixation of up to 3 slide flasks. Melanoma cells were seeded onto 9 cm<sup>2</sup> slide flasks (Nunc, Thermo Fisher Scientific, Langenselbold, Germany) at a density of  $0.2 \times 10^6$  cells per flask and grown for 24 h at 37 °C in the medium described above. After washing with phosphate buffered saline (PBS), flasks were filled completely with phenol red-free DMEM medium containing 0.25 % bovine serum

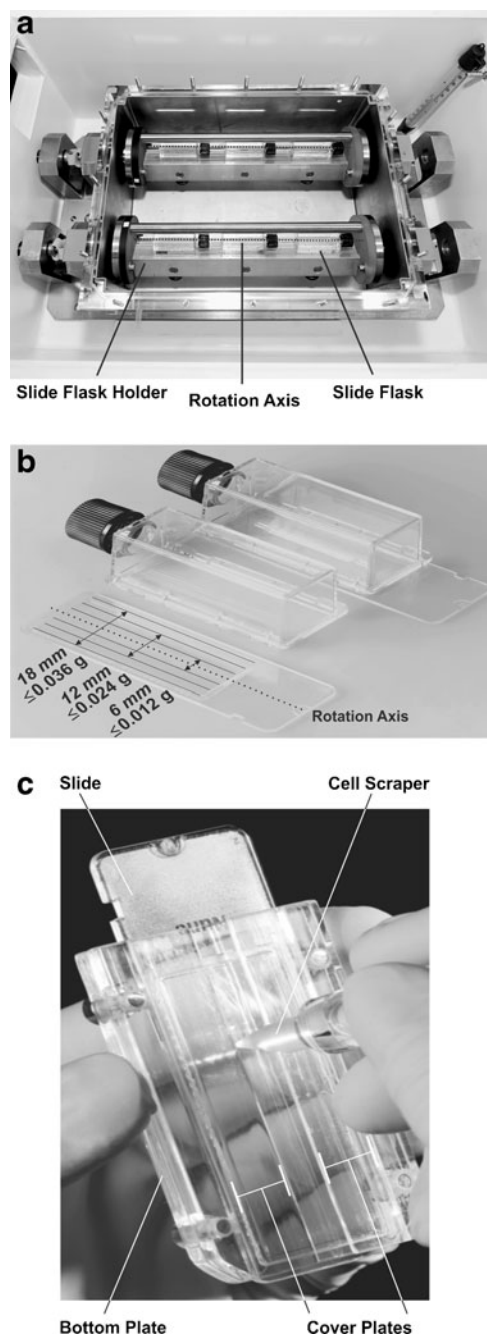


**Fig. 1** 2-D Clinostat adapted for slide flasks and slide chamber for cell collection. **a** 2-D clinostat with slide flask holder for three slide flasks on each rotation axis. **b** Commercially available 9.0 cm<sup>2</sup> slide flask with removable slide. The slides allow investigation of cells from different culture areas exposed to defined maximal residual accelerations, e.g.,  $\leq 0.012$  g,  $\leq 0.024$  g, or  $\leq 0.036$  g (respective slide area with a diameter of 6 mm, 12 mm, or 18 mm). **c** Cell harvesting chamber. Slides are placed in the slide chamber consisting of a bottom plate and two cover plates forming free areas of 6 mm ( $\leq 0.012$  g) or 12 mm ( $\leq 0.024$  g) for collection of cells using an appropriate cell scraper

albumin (BSA), 10 mM 4-(2-hydroxyethyl)-1-piperazine-ethanesulfonic acid (HEPES), pH 7.4 (DMEM-HEPES),

and 0.1 mM 3-isobutyl-1-methyl-xanthine (IBMX), a non-selective phosphodiesterase inhibitor (Ivanova et al. 2004). Cells were incubated for 2 h at 37 °C. Three cell culture slide flasks were inserted per horizontal rotation axis and clinorotated at 60 rpm for 24 h and 37 °C, respectively. The RAW 264.7 cells were seeded at a density of  $1 \times 10^6$  cells per slide flask completely filled with DMEM medium containing 10 % FCS and 1 % penicillin/streptomycin. After 2 h at 37 °C for adherence, 3 slide flasks were inserted per rotation axis of the fast-rotating 2-D clinostat and rotated at 60 rpm for 1 h (37 °C).

For all experiments 1-g controls were prepared simultaneously and placed inside the clinostat box in a horizontal position. Slide flasks with bubbles in the medium were discarded, as clinorotation even with a single bubble induced rounding-up and detachment of cells (data not shown). The loss of adherence of cells as an indicator of detachment was monitored microscopically and quantified by counting the number of adherent cells by subsequent trypsination (0.005 % trypsin/0.02 % EDTA) 24 h after clinorotation using Trypan Blue exclusion assay.

#### Harvesting Device for Adherent Cells Grown in Slide Flasks

In the 2-D clinostat using slide flasks, only a small number of cells are located in the rotation axis, an optimal position for very high quality of simulations. All other cells are exposed to different residual acceleration, depending on the rotation speed and the distance from the rotation center. We investigated the effects of different ranges of residual accelerations on the mRNA levels of guanylyl cyclase A (GC-A), an enzyme catalyzing the synthesis of the second messenger 3', 5'-cyclic guanosine monophosphate (cGMP), in human 1F6 melanoma cells. To collect only cells exposed to defined ranges of g-forces, e.g.  $\leq 0.012$  g,  $\leq 0.024$  g, or  $\leq 0.036$  g, corresponding to a slide flask area with a diameter of 6 mm, 12 mm, or 18 mm (Fig. 1b), respectively, a special harvesting slide chamber was constructed (Fig. 1c). This chamber consists of two cover plates attached to a bottom plate, allowing slide insertion without wiping off the cell layer. The cover plates are designed to form a free area along the slides, whose width in mm depends on the relevant g-values for investigation and functions as a track for corresponding cell scrapers.

#### RNA Isolation and Real-Time Quantitative Polymerase Chain Reaction (qPCR) Analyses

RNA isolation and qPCR analysis were performed as described previously (Ivanova et al. 2011). Briefly, for RNA isolation and gene expression analyses on mRNA level, 1F6 melanoma cells were harvested in areas of  $\leq 0.012$  g,

$\leq 0.024$  g (for both using the harvesting slide chamber), or  $\leq 0.036$  g (from whole slide flask) immediately after stopping the clinostat. In order to obtain sufficient numbers of cells for mRNA analyses, cells from two slide flasks were pooled. Total RNA was isolated from cell lysates using the RNeasy Plus® Micro kit (Qiagen®, Hilden, Germany). Then 1  $\mu$ g of RNA was reverse transcribed into single-stranded cDNA by random priming (QuantiTect® Reverse Transcription system, Qiagen®, Hilden, Germany). As example for investigation of gene expression, cDNA analyses was performed using primers for GC-A, the housekeeping gene glyceraldehyde 3-phosphate dehydrogenase (GAPDH), hypoxanthine phosphoribosyltransferase 1 (HPRT1) (all obtained from QuantiTect® primer, Qiagen®, Hilden, Germany) as endogenous reference and SYBR green as fluorescent dye (QuantiFast® SYBR Green PCR kit, Qiagen®, Hilden, Germany). For negative controls no-template reaction mixes were used. Data were acquired after one PCR initial activation step (5 min at 95 °C) and two-step cycling (40 cycles), each cycle consisting of 10 s denaturation at 95 °C plus combined annealing and extension for 30 s at 60 °C. Levels of gene expression were determined using an efficiency-corrected and calibrator-normalized relative quantification method (LightCycler®, Roche).

#### Cytoskeleton Staining

For investigations on the impact of clinorotation on the cytoskeleton in adherent macrophages, f-actin fibers were stained by Texas Red-conjugated Phalloidin. After stopping of the clinostat, cells (without harvesting) were immediately fixed for 30 min with 4 % paraformaldehyde (PFA), washed in PBS and permeabilized using 0.2 % Triton X-100 in PBS at room temperature (RT). After 1 h blocking with 3 % BSA in PBS cells were incubated in PBS containing 1  $\mu$ g/ml 4-6-diamidino-2-phenylindole-d-hydrochloride (DAPI) (Applichem, Darmstadt, Deutschland) in 0.3 % BSA for nuclei visualization and Phalloidin-Texas Red 1:40 (Invitrogen, Darmstadt, Germany) for 1 h at RT. Samples were washed in PBS and mounted in Fluorescent Mounting Medium (Dako, Hamburg, Germany). Subsequent analysis of 200 cells exposed to a maximum residual acceleration of 0.006 g (area with a diameter of 3 mm) in the adhesion region was performed using an Eclipse 80i Nikon microscope equipped with a confocal imaging system (D-Eclipse C1) with lasers of 408 nm (DAPI) and 543 nm (Texas Red).

#### Result Analyses

Results are presented as means  $\pm$  SEM from 3–5 independent experiments of 4–6 replicates. Means were compared using an unpaired *t*-test. Differences were considered significant when  $P < 0.05$ .

## Results

### Application of Slide Flasks and Harvesting Device for Gene Expression Analyses

Application of the presented slide flasks and slide chamber enabled collection of cells exposed to a defined maximal residual acceleration. As an example for gene expression analyses of 2-D clinorotated adherent cells, we determined GC-A mRNA levels in 1F6 cells exposed to  $\leq 0.012$  g,  $\leq 0.024$  g, or  $\leq 0.036$  g (respective slide area with a diameter of 6 mm, 12 mm, or 18 mm) (Fig. 2) for 24 h. The respective GC-A mRNA levels were  $51.7 \% \pm 3.9 \%$ ,  $83.8 \% \pm 8 \%$ , and  $94.0 \% \pm 3.7 \%$  of 1-g controls in 1F6 melanoma cells, indicating that the down-regulation of the GC-A mRNA levels is inversely proportional to the residual acceleration. Further, the mRNA levels of the housekeeping gene GAPDH were not altered for the investigated range of g-forces. The 1F6 human melanoma cells exposed on a fast-rotating 2-D clinostat (60 rpm) were viable during the investigated time periods of 24 h. The percentages of the necrotic cells were less than 2.5 % of the total cell number.

### Application of Slide Flasks for Staining Analyses

Using laser scanning microscopy and a Phalloidin-Texas Red staining procedure, we investigated the f-actin filament system at the adhesion region after 1 h exposure to clinorotation ( $\leq 0.006$  g) in comparison to static 1-g controls. Representative images are given in Fig. 3. A large

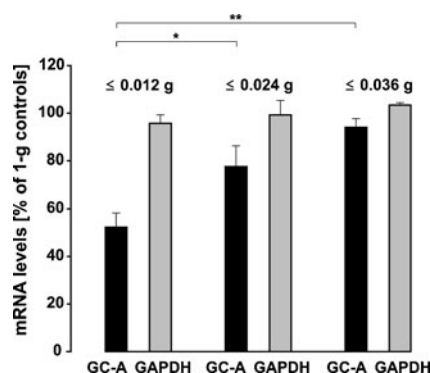


**Fig. 2** Influence of maximal residual accelerations of  $\leq 0.012$  g,  $\leq 0.024$  g, and  $\leq 0.036$  g on the expression of GC-A and the housekeeping gene GAPDH in low-metastatic 1F6 human melanoma cells. The investigated cells were clinorotated for 24 h at 37 °C. The mRNA levels of GC-A (black bars) and GAPDH (grey bars) were determined by a calibrator-normalized and efficiency-corrected real-time quantitative polymerase chain reaction, using HPRT1 as an internal reference. Results are presented as percent of 1-g controls. Data are means of 4–6 replicates of 3–5 independent experiments. Asterisks (\*/\*\*) indicate statistically significant differences ( $P < 0.05$  /  $P < 0.01$ ) between cells exposed to g-values  $\leq 0.024$  g or  $\leq 0.036$  g and cells exposed to  $\leq 0.012$  g

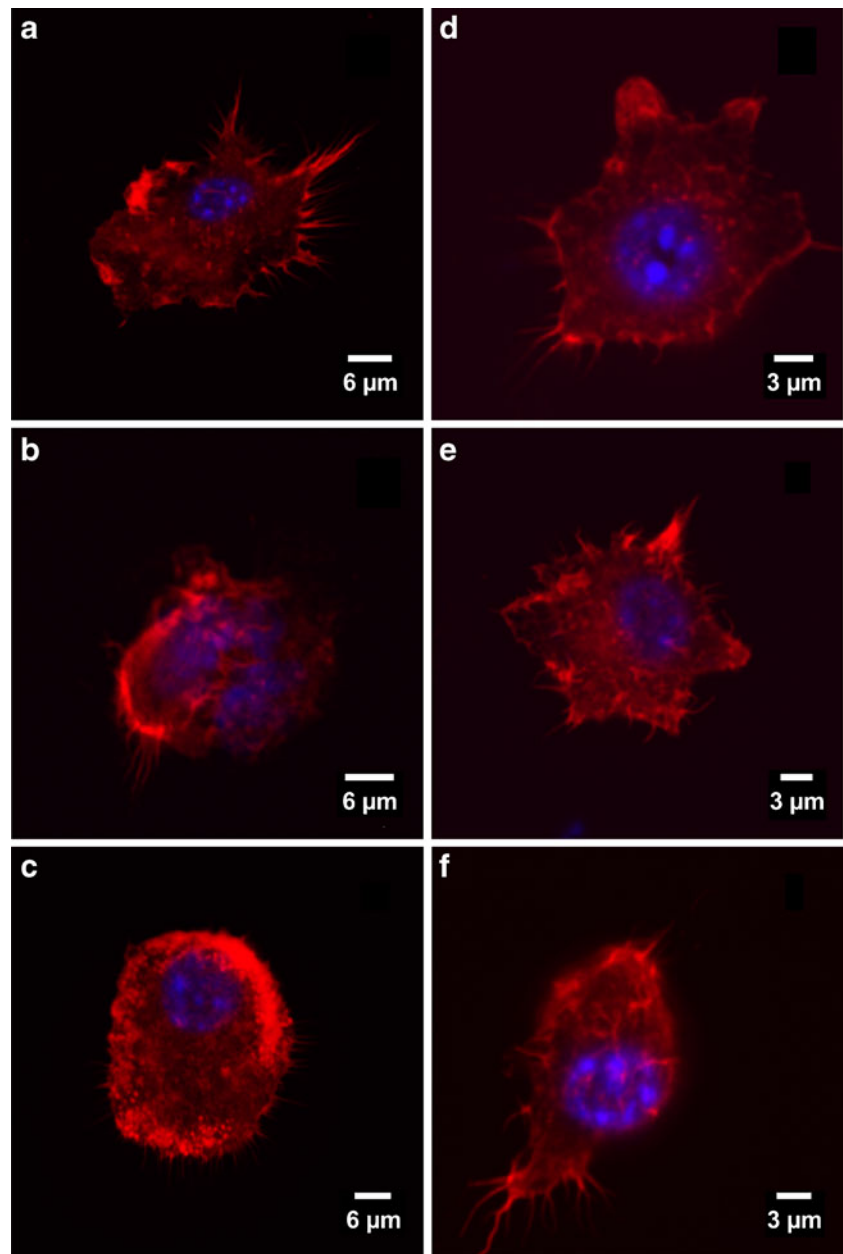
variety of cell forms and f-actin arrangements was observed, in which f-actin is accumulated particularly in the pseudopodia of 2-D clinorotated cells (Fig. 3a) as well as of 1-g controls (Fig. 3d, e and f). Stress fibers of the actin filament system were also found in macrophages under both conditions—clinorotation and at 1 g. However, clinorotated cells appeared larger and flattened compared to the 1-g control cells. These results indicate that under the investigated conditions 1 h of clinorotation induces changes in the size of adherent macrophages, but obviously not in the f-actin filament system.

## Discussion

In this study we demonstrate the adaptation of a 2-D clinostat for experiments with adherent cells using commercially available slide flasks. As clinorotation generates centrifugal forces, which depend on the cell's distance from the rotation axis and the rotation speed, a gradient of residual acceleration is present in the respective flasks. Taking this into account, we constructed an appropriate slide chamber for harvesting of adherent cells exposed to defined maximal residual accelerations followed by analyses.

To test the application of slide flasks and the harvesting slide chamber for gene expression analysis, we investigated the effects of clinorotation on the expression of GC-A, as the presence of functional natriuretic peptide-sensitive membrane-bound guanylyl cyclase isoforms (e.g., GC-A and GC-B) in melanoma cells has been related to metastasis (Ivanova et al. 2001; Kong et al. 2008). Moreover, we previously reported a down-regulation of the mRNA levels of GC-A and GC-B in human low metastatic 1F6 and highly metastatic BLM melanoma cells exposed to  $\leq 0.012$  g for 6 h and 24 h in comparison to static 1-g controls (Ivanova et al. 2011), suggesting a reduction of the metastatic potential of melanoma cells. Here, we present a new set of experiments in order to study the effect of different ranges of residual accelerations (e.g.,  $\leq 0.012$  g,  $\leq 0.024$  g, or  $\leq 0.036$  g for 24 h) on the mRNA levels of GC-A in human 1F6 melanoma cells. We found a down-regulation of GC-A mRNA levels in clinorotated 1F6 melanoma cells of approximately 50 % for residual accelerations  $\leq 0.012$  g and of approximately 18 % for  $\leq 0.024$  g compared to 1-g controls, respectively. There were no changes at  $\leq 0.036$  g. In addition, the value for the area of  $\leq 0.012$  g is similar to previously published data (Ivanova et al. 2011). As the cells experienced compatible physical and environmental conditions in spite of gravity, the results indicate a threshold of gravisensatation in melanoma cells. Together, our data show a clear relationship between residual acceleration and gene expression within the same experimental set-up. We assume that the maximal effect in our studies at  $\leq 0.012$  g may

**Fig. 3** Influence of 2-D clinorotation on the f-actin filament system in adherent RAW 264.7 macrophages. Representative laser scanning micrographs of cells exposed for 1 h up to 0.006 g (diameter of 3 mm) (a–c) and of the corresponding 1-g controls (d–f) are shown. The f-actin filaments were stained by Phalloidin-Texas Red (*bright red regions*) and the nuclei by DAPI (*blue regions*), respectively. Scale bars are 6  $\mu\text{m}$  for clinostat experiments and 3  $\mu\text{m}$  for 1-g controls, demonstrating the increase of clinorotated cells



correspond to the expected behavior in real microgravity, but it has still to be tested in appropriate flight experiments.

We also tested the application of slide flasks for investigations of possible effects of clinorotation on highly dynamic intracellular structures, e.g., alterations of the cytoskeletal elements in a very high quality area of simulation (e.g.,  $\leq 0.006$  g) using another cell type, e.g., RAW 264.7 macrophages. We found an increase of cell size for clinorotated cells ( $\leq 0.006$  g for 1 h) in comparison to 1-g controls, which could be related to spreading and flattening accompanied by the formation of additional focal contacts, when the g-vector cannot be detected anymore by the cells. Interestingly, no alteration of the f-actin filament system in RAW 264.7 macrophages comparing 2-D clinorotated

cells ( $\leq 0.006$  g for 1 h) and 1-g controls was evident after 1 h of clinorotation. In contrary, changes in the f-actin filament system and cell morphology have been demonstrated in several cell type such as osteoblasts exposed to real microgravity (Hughes-Fulford 2003) and cells of the human monocyte cell line J-111 exposed to real microgravity and on a random positioning machine (Meloni et al. 2006, 2011).

For osteoblasts, alterations in the actin cytoskeleton and loss of focal adhesions have been found after 4 days in microgravity in comparison to flown cells under 1-g conditions (Hughes-Fulford 2003). The discrepancy between osteoblast and RAW 264.7 macrophages could be attributed to the differences in their motility. In contrary to osteoblasts,



**Fig. 4** New clinostat set-up, which can be used as insert for incubators. The clinostat set-up is equipped with 6 parallel rotating axes that can be loaded with 24 slide flasks in total (Design M. Görög, Institute of Aerospace Medicine, DLR, Cologne, Germany)

which are not motile, the f-actin filament system of macrophages is constantly rearranged for cellular movement. We also explain the discrepancies in the results due to the fact that cytoskeletal rearrangements are highly dynamic processes, which demand on-line fixations and on-line visualization during clinorotation; otherwise the effect might have already disappeared or misinterpreted with respect to adaptation phenomena. By using a clinostat microscope (Hemmersbach et al. 2006) and thus on-line visualization, we observed dynamic changes in the RAW 264.7 cell morphology – rounding up of the cells followed by flattening (data not shown), finally resulting in our observation of an increased cell size after clinorotation. Thus, we confirm the data of Moes et al. (2011) who also stated comparable dynamical changes in the morphology and actin filament system of the human epidermoid cell line A431 in simulated (clinostat) as well as real microgravity (sounding rocket) conditions.

For monocyte J-111 cells, Meloni et al. (2006) stated significant changes in the structure of f-actin,  $\beta$ -tubulin and vinculin after 1 h and 24 h exposure on a random positioning machine in comparison to 1-g controls and after 24 h exposure of J-111 cells in real microgravity on the ISS (Meloni et al. 2011) compared to 1-g in-flight and ground controls, which are related to the highly reduced motility of monocytes in low gravity (Meloni et al. 2011). Whether differences between our results and the already published data obtained by just two endpoint measurements at 1 h and

24 h are due to cell specific responses and sensitivities to altered gravity or just due to operational differences have to be shown in the future.

Current hardware developments (Institute of Aerospace Medicine, DLR, Cologne, Germany) will enlarge the experimental challenges of gravity-related experiments in ground based facilities. In this context, a new clinostat set-up with 6 parallel rotating axes (24 slide flasks in total) has been constructed as insert for commercially available incubators (Fig. 4), which will increase the amount of exposed material close to the center of rotation and thus in the area of simulated microgravity conditions. In addition, such kind of device will allow fixation at dedicated time lines, providing more information on gravity-related changes in a highly dynamic and adaptive systems such as the cytoskeleton.

Taken together, our experimental approach opens a lot of possibilities with respect to experiments under altered gravitational stimulation aiming to achieve simulated microgravity conditions. Commercially available slide flasks can be used for exposition of adherent cells in a 2-D clinostat and provide optimal growth conditions up to 24 h as revealed by the viability of the exposed cells. Longer lasting experiments are principally possible, but then a culture medium change is needed. Our device is ideally suited to investigate processes, which need to develop and remain stable for some time, e. g., gene expression. However, in the case of fast and highly dynamic processes on-line visualization and fixation should at least additionally be performed, otherwise adaptation phenomena could be masked. Due to the residual acceleration gradient present in the slide flasks during 2-D clinorotation, the ranges of maximal g-values have to be considered, discussed and adjusted to the investigated adherent cell type and to the applied analyses. Finally, simulation studies need to be verified in real microgravity allowing the usage of the term “simulated microgravity” for this kind of cell system.

**Acknowledgments** The present study was supported by the Program Directorate of Human Spaceflight, DLR, Cologne, Germany. The authors acknowledge that this study forms a part of a Ph.D. thesis of Peter Eiermann (Helmholtz Space Life Sciences Research School at the German Aerospace Center, Institute of Aerospace Medicine, Cologne, Germany), and the Bachelor thesis of Sascha Kopp (University of Applied Science, Bonn-Rhein-Sieg, Germany).

## References

- Briegleb, W.: A model for weightlessness-simulation using microorganisms. *Naturwissenschaften* **54**, 167 (1967)
- Briegleb, W.: Some qualitative and quantitative aspects of the fast-rotating clinostat as a research tool. *ASGSB Bull.* **5**, 23–30 (1992)

- Brungs, S., Hauslage, J., Hilbig, R., Hemmersbach, R., Anken, R.: Effects of simulated weightlessness on fish otolith growth: clinostat versus rotating-wall vessel. *Adv. Space Res.* **48**, 792–798 (2011)
- Hemmersbach, R., Von der Wiesche, M., Seibt, D.: Ground-based experimental platforms in gravitational biology and human physiology. *Signal Transduct.* **6**, 381–387 (2006)
- Herranz, R., Anken, R., Boonstra, J., Braun, M., Christianen, P.C., de Geest, M., Hauslage, J., Hilbig, R., Hill, R.J., Lebert, M., Medina, F.J., Vagt, N., Ullrich, O., van Loon, J.J., Hemmersbach, R.: Ground-based facilities for simulation of microgravity: organism-specific recommendations for their use, and recommended terminology. *Astrobiology* **13**, 1–17 (2013)
- Hughes-Fulford, M.: Function of the cytoskeleton in gravisensing during spaceflight. *Adv. Space Res.* **32**, 1585–1593 (2003)
- Hughes-Fulford, M., Lewis, M.L.: Effects of microgravity on osteoblast growth activation. *Exp. Cell Res.* **224**, 103–109 (1996)
- Ivanova, K., Le Poole, I.C., Gerzer, R., Westerhof, W., Das, P.K.: Effect of nitric oxide on the adhesion of human melanocytes to extracellular matrix components. *J. Pathol.* **183**, 469–476 (1997)
- Ivanova, K., Das, P.K., van den Wijngaard, R.M., Lenz, W., Klockenbring, T., Malcharzyk, V., Drummer, C., Gerzer, R.: Differential expression of functional guanylyl cyclases in melanocytes: absence of nitric-oxide-sensitive isoform in metastatic cells. *J. Invest. Dermatol.* **116**, 409–416 (2001)
- Ivanova, K., Zadeh, N.H., Block, I., Das, P.K., Gerzer, R.: Stimulation of cyclic GMP efflux in human melanocytes by hypergravity generated by centrifugal acceleration. *Pigm. Cell Res.* **17**, 471–479 (2004)
- Ivanova, K., Eiermann, P., Tsiokas, W., Hauslage, J., Hemmersbach, R., Gerzer, R.: Natriuretic peptide-sensitive guanylyl cyclase expression is down-regulated in human melanoma cells at simulated weightlessness. *Acta Astronaut.* **68**, 652–655 (2011)
- Klaus, D.M., Todd, P., Schatz, A.: Functional weightlessness during clinorotation of cell suspensions. *Adv. Space Res.* **21**, 1315–1318 (1998)
- Kong, X., Wang, X., Xu, W., Behera, S., Hellermann, G., Kumar, A., Lockey, R.F., Mohapatra, S., Mohapatra, S.S.: Natriuretic peptide receptor a as a novel anticancer target. *Canc. Res.* **68**, 249–256 (2008)
- Meloni, M.A., Galleri, G., Pippia, P., Cogoli-Greuter, M.: Cytoskeleton changes and impaired motility of monocytes at modelled low gravity. *Protoplasma* **229**, 243–249 (2006)
- Meloni, M.A., Galleri, G., Pani, G., Saba, A., Pippia, P., Cogoli-Greuter, M.: Space flight affects motility and cytoskeletal structures in human monocyte cell line J-111. *Cytoskeleton* **68**, 125–137 (2011)
- Moes, M.J.A., Gielen, J.C., Bleichrodt, R.J., van Loon, J.J.W.A., Christianen, P.C.M., Boonstra, J.: Simulation of microgravity by magnetic levitation and random positioning: effect on human A431 cell morphology. *Microgravity Sci. Technol.* **23**, 249–261 (2011)
- Raschke, W.C., Baird, S., Ralph, P., Nakoinz, I.: Functional macrophage cell lines transformed by Abelson leukemia virus. *Cell* **15**, 261–267 (1978)
- Thiel, C.S., Paulsen, K., Bradacs, G., Lust, K., Tauber, S., Dumrese, C., Hilliger, A., Schoppmann, K., Biskup, J., Golz, N., Sang, C., Ziegler, U., Grote, K.H., Zipp, F., Zhuang, F., Engelmann, F., Hemmersbach, R., Cogoli, A., Ullrich, O.: Rapid alterations of cell cycle control proteins in human T lymphocytes in microgravity. *Cell Commun. Signal* **10**, 1 (2012)
- Ulbrich, C., Pietsch, J., Grosse, J., Wehland, M., Schulz, H., Saar, K., Hubner, N., Hauslage, J., Hemmersbach, R., Braun, M., van Loon, J., Vagt, N., Egli, M., Richter, P., Einspanier, R., Sharbati, S., Baltz, T., Infanger, M., Ma, X., Grimm, D.: Differential gene regulation under altered gravity conditions in follicular thyroid cancer cells: relationship between the extracellular matrix and the cytoskeleton. *Cell. Physiol. Biochem.* **28**, 185–198 (2011)